A national laboratory of the U.S. Department of Energy
Office of Energy Efficiency & Renewable Energy

National Renewable Energy Laboratory

Innovation for Our Energy Future

Solar Cell Design for Manufacturing

Final Report
October 2005 — September 2007

J.A. Rand
GE Energy, LLC
Newark, Delaware

Subcontract Report
NREL/SR-520-43228
May 2008

NREL is operated by Midwest Research Institute • Battelle Contract No. DE-AC36-99-GO10337

Solar Cell Design for Manufacturing

Final Report
October 2005 — September 2007

J.A. Rand
GE Energy, LLC
Newark, Delaware

NREL Technical Monitor: Richard L. Mitchell

Prepared under Subcontract No. ZAX-5-33628-06

Subcontract Report
NREL/SR-520-43228
May 2008

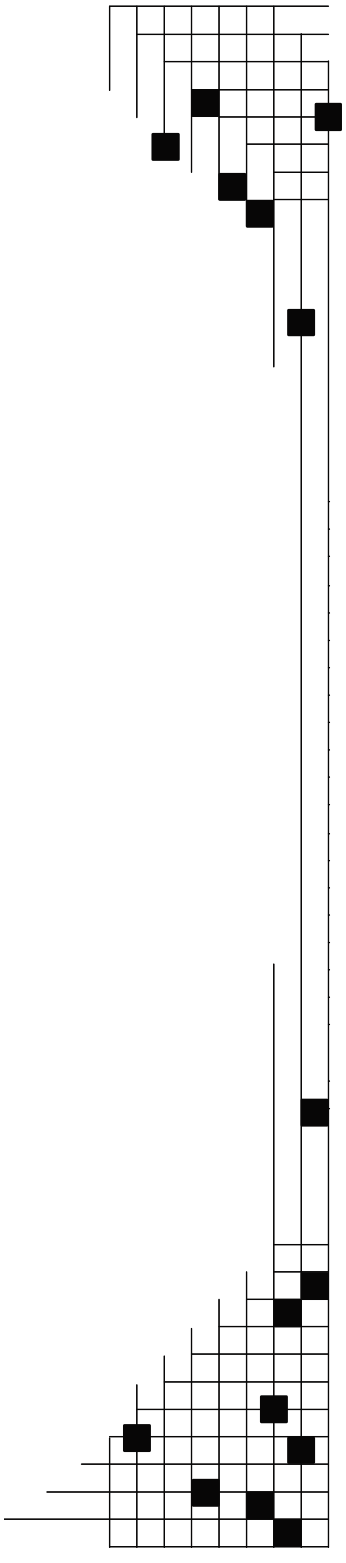

National Renewable Energy Laboratory
1617 Cole Boulevard, Golden, Colorado 80401-3393
303-275-3000 • www.nrel.gov

Operated for the U.S. Department of Energy
Office of Energy Efficiency and Renewable Energy
by Midwest Research Institute • Battelle

Contract No. DE-AC36-99-GO10337

Executive Summary

The use of silicon based photovoltaic systems has become more widespread in recent years; however, prices and presumably cost for manufacturing silicon based PV modules have not dropped. That costs for silicon based solar cells remain high is due in part to the high cost of manufacturing for silicon wafers. While silicon wafer manufacturers have been successful in reducing wafer thickness by almost 50% from about 340μm to 180μm going forward this approach is one of diminishing returns due to the cost of wafer sawing and the large kerf loss, which is currently approaching 50%. New concepts in wafer manufacturing are necessary in order to control costs.

Under this DOE program, GE is improving its molded wafer process. The approach taken by GE is to leverage the inherent advantages of molded wafers and mitigate the disadvantages. Advantages include the very low cost of wafer making, the practical absence of inherent silicon losses, the low demands on feedstock quality and the ability to shape wafers to any desired form. The main disadvantages are relatively low solar cell efficiency and high wafer thickness.

During Phase II of this year, we focused our efforts primarily towards improving solar cell efficiency, development of our metal wrap through process, and roof integrated module. GE acquired a new 15MW molded wafer furnace, which arrived early in 2007.

During this program, significant progress was made in improving our solar cell process, developing our metal wrap through process and completing highly accelerated lifetime testing on elements of our roof integrated module. Specifically, an improved diffusion process that results in near ideal blue response at moderately low emitter sheet resistance of 50 to 60Ohms/square was developed. This is particularly important for our molded wafer development since long wavelength response is limited.

This report covers only half of the Phase II activities originally planned for this effort. During Phase II, GE Energy (USA), LLC kicked off a SAI-TPP contract. The work contained in the remainder of the contract reported on here has been transferred to the SAI contract.

Table of Contents

1. Task 5 - Advanced Module Manufacturing – All Back Interconnect Modules

1.1 Introduction

All back contact modules made with metal wrap through (MWT) solar cells promise up to 10% relative higher module efficiency for a given starting wafer quality. The efficiency gain results from a combination of increased solar cell performance due to reduced front side shading, reduced resistive (I^2R) loss in the module interconnections and tabbing and a better utilization of the module area due to the elimination of exposed busing between strings. We have identified the MWT approach as a very good fit with our molded wafer technology. During the second phase of this contract, we focused on the development of a packaging, assembly, and high-volume manufacturing method for solar panels fabricated using back-side contact photocells and an interconnect system. As part of their technology development effort for this project the GE Global Research (GEGR) team has created a preliminary design of a backplane interconnection method and evaluated interconnect materials. The next step is the optimization of process parameters and fabrication of prototype laminates for functional and mechanical testing.

1.2 Interconnect Process

The molded wafer PV cells are 156mm x 156mm x 600μm, trimmed, with sixteen laser-cut through-holes. The through-holes (when coated with ink) provide for conduction of the charge from the top (n-type) of the PV cell to the bottom of the PV cell. The through-holes provide a method for the I/O pads to be located on the backside of the PV cell; this I/O configuration eliminates shadowing, a condition that occurs in the conventional methods used to interconnect I/O located on the active (top) side of the PV cell, and provides for potentially higher reliability of the electrical interconnect (cell-to-cell).

During Phase I, the material system requirements to adhere MWT solar cells to a patterned conductor (see Figure 1) were established and highly accelerated lifetime testing was started and, for some materials, completed.

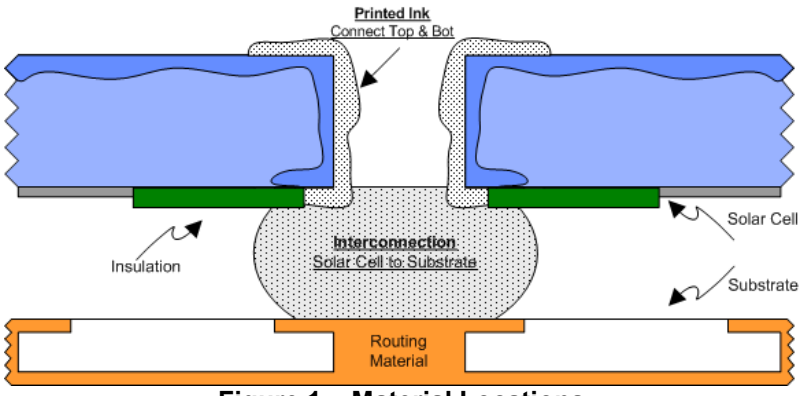

Figure 1 – Material Locations

In Phase II, the focus was primarily on determining manufacturability and optimal interconnect design. To reduce the number of process steps required in assembling a MWT module, it is desirable to combine the curing of conductive adhesive with the lamination process. We identified a conductive adhesive with potentially suitable properties (see Table 1) and tested it using a co-lamination process.

Material Property	Value
Cure Process	15 minutes at 150°C
Glass Transition Temperature (Tg)	≥ 100°C
Coefficient of Thermal Expansion (CTE) below Tg	24 x 10-6 in/in/°C
Storage Modulus	311,866 psi
Volume Resistivity	≤ 0.0005 Ohm-cm
Pot Life	24 Hours
Continuous Operating Temperature	- 55°C to 200°C

Table 1 – Material Properties of Conductive Adhesive

Since both the EVA and the adhesive are curing in the same step, it was necessary to evaluate the cure kinetics of both materials. The objective of this study was to investigate whether the adhesive interconnect formation was in any way inhibited by the surrounding EVA during the lamination process. The viscosities of the EVA and the adhesive were measured across the lamination temperature profile using parallel plate rheometry (as shown in Figure 2). Figure 3 shows the results of the test. It was found that the EVA begins to flow after the adhesive joint formation has taken place. As a result, there is no mixing of the EVA and the adhesive, nor is there any displacement of the adhesive by the liquid EVA.

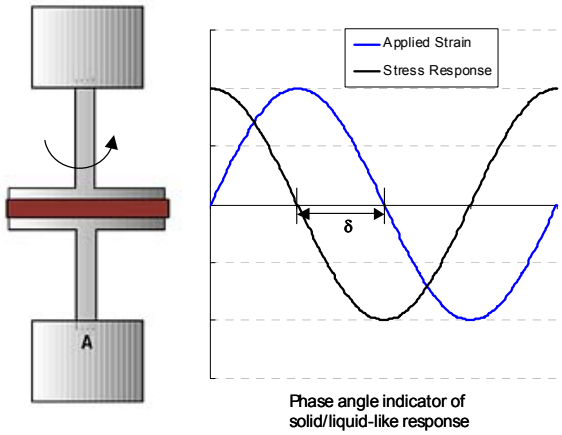

Figure 2 – Schematic of Parallel Plate Rheometry

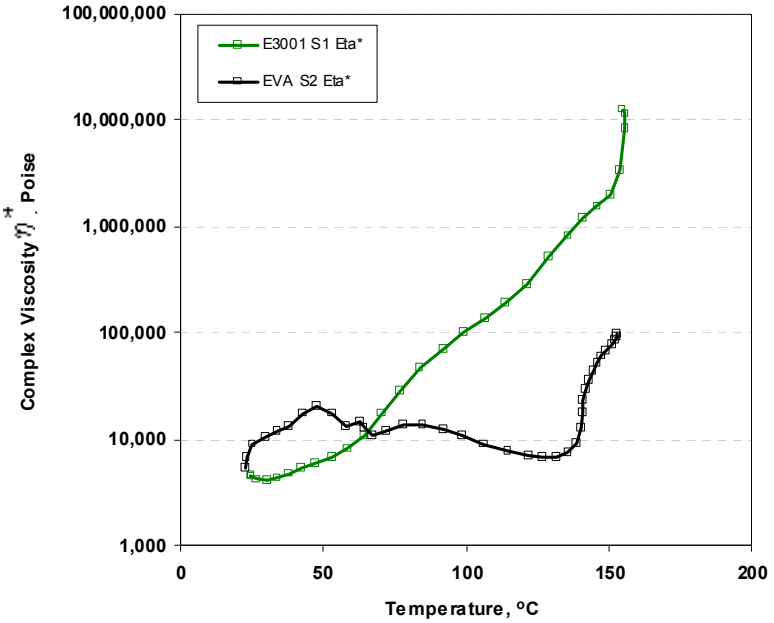

Figure 3 – Results from Parallel Plate Rheometry

The impact due to air-air thermal shock (AATS) cycling was assessed over 320 cycles between temperature limits of –40°C and 85°C with a dwell time of 10 minutes at each limit. The electrical resistance was measured at regular cycling intervals. It was observed that the interconnect resistance dropped by about 18% over the 320 cycles (Figure 4). It is likely that the drop in resistance is due to continued crosslinking in the adhesive across the thermal cycles. The shear strength of the interconnect joints was measured at the end of thermal cycling. An average value of 842 psi was measured for 12 samples; the average shear strength measured exceeded the desired value of 500 psi. Similarly, an average

shear strength of 950 psi was measured for 18 samples that were exposed to 85%RH at 85°C for 1000 hours.

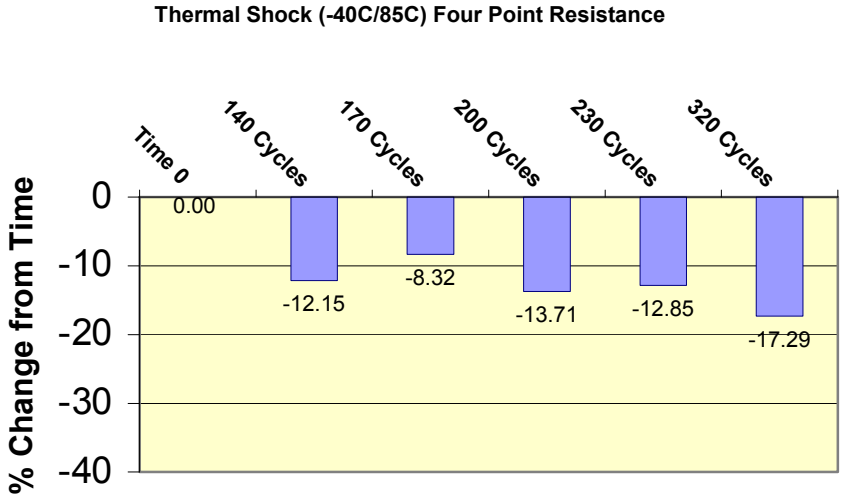

Figure 4 – Results from Parallel Plate Rheometry

1.3 Insulation

Since the MWT cell places both p-type and n-type connections in the same plane on the back of the cell, it becomes necessary to isolate the charge on the front-side conductor from the back of the cell. GEGR has investigated several methods of dielectric application to achieve this.

Earlier, in Phase I, it was assumed that a dielectric sheet could be inserted between the conductor and the back of the cell. The sheet could have an adhesive to hold it in place. One of the materials tested was a Mylar sheet, 7-10 mil thick. In addition to being bulky, the material introduced undesirable effects and potential risks. There was some concern that the interconnect material could get underneath the dielectric sheet and cause a short. Another concern was that during lamination, the EVA could flow underneath and disrupt joint formation. In addition, the cost of the material was higher than desired.

Later a printable dielectric material was tested. The result was a one-part, 2 mil thick, screen printable, insulation layer. The material is approximately 75% lower in cost than the dielectric sheet concept and design changes are highly adaptable. This material required approximately 45 minutes at 135°C to cure.

In Phase II, in an effort to optimize the processing time of the dielectric material, a UV-curable version was identified and tested. UV cure times can be less than one minute as compared to the 45 minutes required of thermally cured materials.

These UV curable materials are screen-printable and are widely used in the printed circuits industry. The UV curable insulation materials were cured under a 600 W UV lamp. The insulation passed a voltage leak test from 0 to 100 V DC.

The material was also exposed to 200 cycles of AATS between –40 °C and 85 °C with a dwell time of 10 minutes at each temperature limit. The voltage leakage test was repeated at the end of cycling and no degradation in the material was found.

1.4 Routing

Throughout Phase I, the routing material of choice has been copper, between 5 and 20 mils thick and 100 to 200 mils wide. Copper was chosen as the interconnect material due to its high electrical conductivity, availability, and low cost.

During Phase II of the program, as shown in Figure 5, the cellular insulation pattern was altered, slightly. The insulation printed for the outer fingers was enlarged to accommodate a second design of copper patterns that allows making 90° turns in the cell-to-cell routing path. An example of how this is employed can be seen in Figure 6, showing the routing on a 4-cell, 2x2 module.

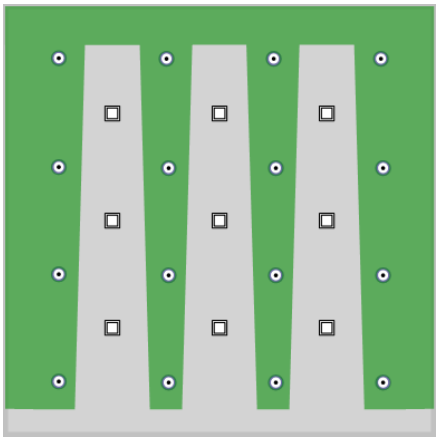

Figure 5 – Enlarged Insulation Print

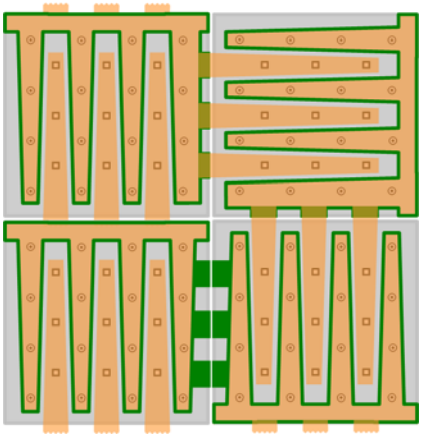

Figure 6 – 2x2 Module With Both Straight and 90° Conductors

1.5 Conventional Cells in Back Plane Package

Due to the long lead times required for developing a metal wrap through cell it was proposed to package conventional screen printed H-bar front contact cells using a metal wrap around (MWA) approach. It was proposed that manufacturing costs could be lowered due to the all back interconnect design as well as some reduction in I^2R loss could be achieved due to the use of larger cross-section conductors on the back.

Modeling was used to examine the feasibility of a back plane interconnect process using H-bar solar cells. Figure 7 details the quantity of copper used versus the corresponding power loss for a conventionally strung design, the MWT, and MWA technologies. According to the model, the power gain benefits of implementing a MWT or MWA technology outweigh the additional copper cost, even at historically high copper prices. However, for a MWA approach, a rectangular (or half size) cell would work far better than the conventional square solar cell.

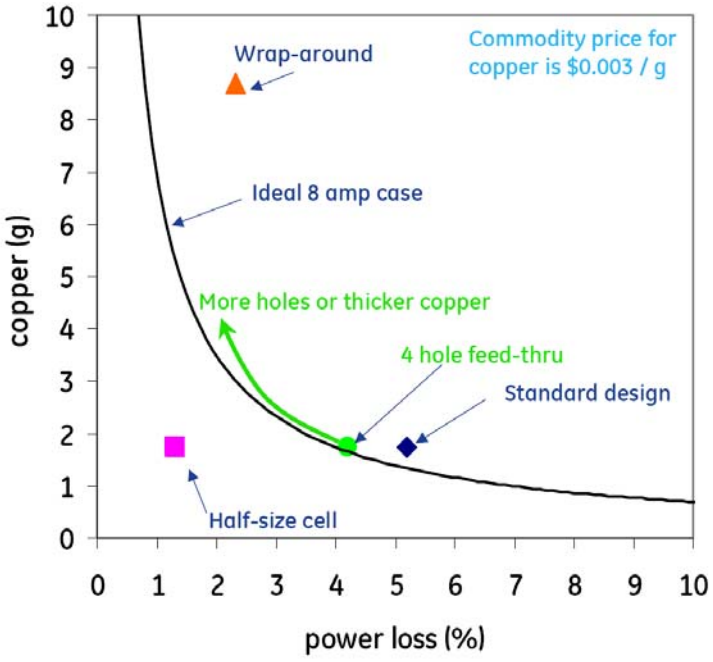

Figure 7 - Grams of copper used in bussing versus associated power loss for H-bar, MWT, and MWA assemblies

Based on modeling results, several design concepts were evaluated. Figure 8 shows two MWA designs: a MWT, and a conventional H-bar design. All designs were individually modeled. The results show that MWA designs have greater shading losses than MWT designs. Reinforcing the front of the wrap-around cells with copper ribbon can rectify this condition.

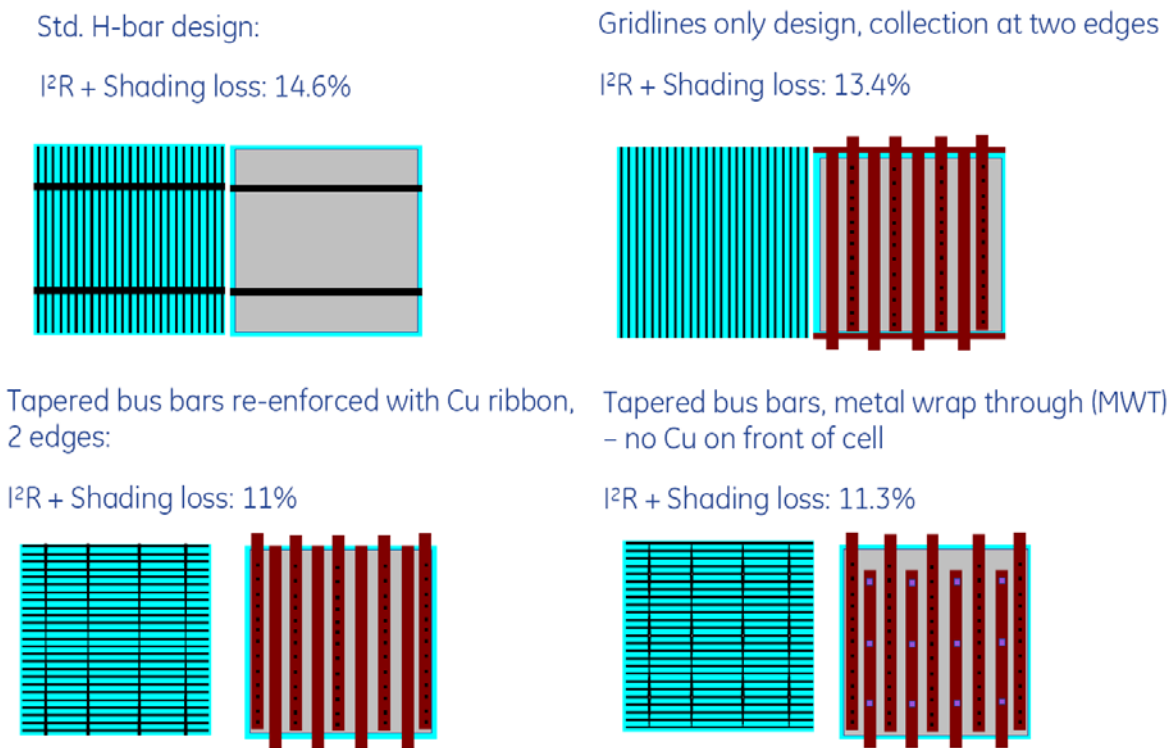

Figure 8 - Front and back layout of two metal wrap-around designs, a standard H-bar design and a metal wrap-through design.

While MWA technology could be implemented to reduce resistive losses in the module package, it was concluded that copper reinforcement on the front of the cell would be required. The copper reinforcement would complicate the process and would be more costly than the current stringing process. Additionally, masking of the copper busing on the front of the cell would be required.

MWT has similar I^2R + Shading losses as reinforced Cu ribbon MWA designs without the addition of copper on the front of the cell.

1.6 Manufacturability

Figure 9 shows the assembly process that had been conceptualized in Phase I. The proposed process flow was evaluated for potential shortcomings through discussions with the manufacturing experts at GEGR and GE Energy.

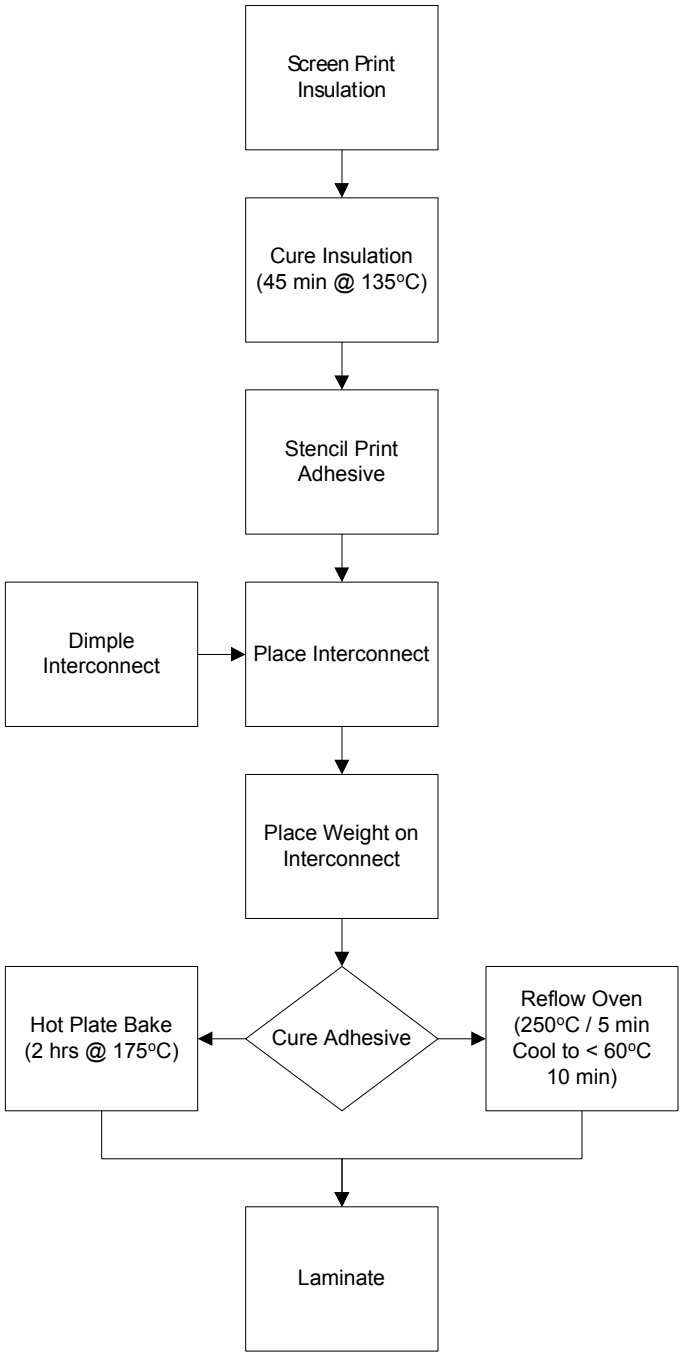

Figure 9 – Previous Process Flow for Back-Contact Assembly

The assembly process begins with screen-printed MWT solar cells. The first step is to screen print the insulation on the cells. The insulation is then thermally cured for 45 minutes at 135°C. The insulated cells are then transferred to the stencil printer for application of the conductive adhesive on to the contact pads. After stencil printing, the cells are placed in an array to create a module. A non-conductive, snap-cure adhesive is then dispensed at key locations. The patterned routing foils are then placed on the cells. The non-conductive adhesive

is cured to hold the routing in place and avoid any movement during subsequent handling.

The cells are then held under pressure, at an elevated temperature (175°C for 2 hours), between two compliant substrates, to cure the conductive adhesive. During this lamination process, the conductive adhesive cure is concurrent with completion of the module lamination. The cells will be inspected for positional accuracy of the printed insulation layer, the printed adhesive, and the routing pattern. The possibility of testing the module prior to lamination is being explored.

In Phase II (see Figure 10), several variables were changed in an effort to shorten the assembly process. It was decided that a UV curable insulation material would be a more suitable option to support the throughput requirement of the assembly process. Thermally curable insulation requires approximately 45 minutes of curing; UV curable material reduces cure time to approximately 40 seconds (a factor of almost 68X). Use of UV curable material requires the purchase of a conveyorized UV curing system (instead of a thermal batch oven, as used for curing thermally curable insulation).

The cost of a UV curing system with its maximum capacity meeting the throughput requirements is approximately $30,000. These systems provide curing under positive pressure as opposed to vacuum, therefore providing the ability to cure in filtered air. Prices include 600 watts/inch high power 10-inch lamps, power supplies, conveyors, and exhaust and cooling blowers.

Another optimization to the process includes a change in conductive adhesive, as discussed in section 1.2. The new conductive adhesive cures within a similar time/environment to the process parameters of the lamination process. The ability to cure the adhesive within 15 minutes at 150°C is a more practical approach and allows for combination with the lamination procedure. This not only eliminates an assembly step, but also eliminates approximately 2 additional hours of processing time and the need to purchase additional curing equipment.

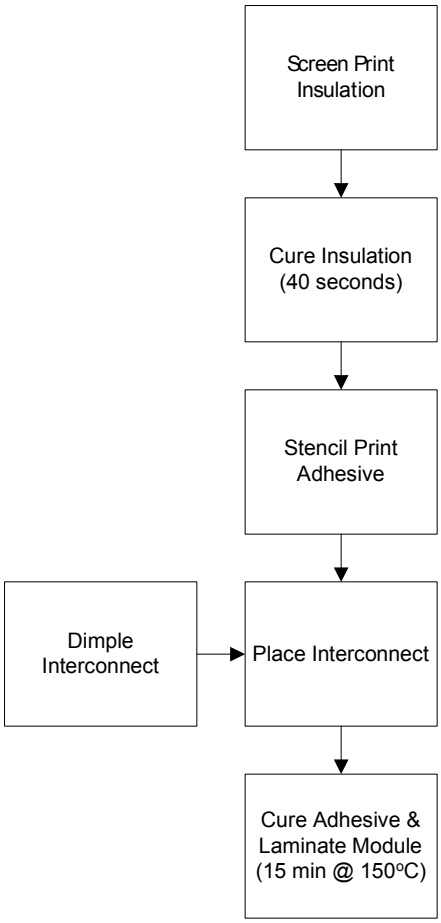

Figure 10 – Current Process Flow for Back-Contact Assembly

1.7 Equipment

Figure 11 and Table 2 show the details of the equipment that will be required for the assembly of the back-contact modules. A throughput requirement of 1200 cells/hour has been assumed. This translates to 22 modules (54 cells per module) per hour at 90% yield.

The printing of the insulation and the conductive adhesives will each require a dedicated screen printer and stencil printer, respectively. The screen printer must have vision capability to align the cells, using fiducials. An integrated inspection system on the printer will eliminate the requirement of a dedicated inspection tool. Note that in this case, there is no major difference between a screen printer and a stencil printer. For all intents and purposes, throughout this report, the two pieces of equipment are identical thus the names may be used interchangeably.

One conveyorized UV cure system will be required to support the target throughput. A customized placement machine will be built to place the routing patterns. If the tacking material is a non-conductive adhesive (materials have yet to be evaluated), a standard dispenser can be used for application. Alternatively, a dispenser can be integrated into the placement equipment. The placement equipment may require the capability to pick and place sheets of glass, EVA and TPE to create the stack-up for lamination. An additional small UV curing setup may be required for the non-conductive tacking adhesive.

The equipment list does not include a laminator. The list also does not include other necessary apparatus such as cell banks and conveyors. The possibility of having dedicated automatic optical inspection tools has been suggested, but is not required. An inspection tool can be a centrally located piece of equipment to inspect the dimensional and positional accuracies of the insulation, adhesives and the patterns. The tool will require appropriate pattern recognition capabilities. If a test step prior to lamination is introduced, then the necessary electrical tooling must be added to the placement tool. Adding a piece of equipment, such as an inspection/test station, warrants an analysis of the cycle time associated with the placement, stack-up, dispensing, and testing of the assemblies in relation to the throughput requirements.

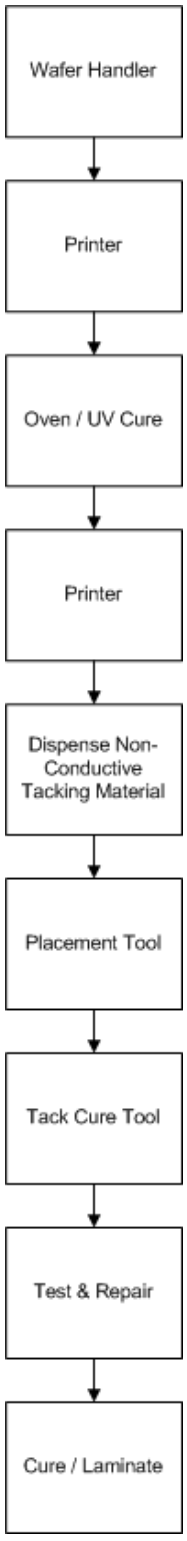

Figure 11 – Equipment Requirement

Equipment Name	Capability
Screen Printer for Insulation	Vision, Integrated Inspection
UV Cure System	High Throughput
Stencil Printer for Conductive Adhesive	Vision, Integrated Inspection
Dispenser	Vision, Integrated Inspection
Placement Tool	Vision, Placement of Routing, EVA & TPE
Automated Optical Inspection (AOI)	High Throughput, Pattern Recognition

Table 2 – List of Equipment and Estimated Costs (total cost for 20 MW line would be <1MM)

1.8 Summary

A complete material system to package MWT solar cells into 54 cell modules using conductive adhesive and printed isolation layers has been developed and all components of the system have been tested for reliability using highly accelerated lifetime tests. Further, an assembly line to produce 20MW of MWT modules has been conceptualized and researched.

2. Task 6 - Solar Cell Manufacturing Cost Reduction - Metallization

2.1 Introduction

The main differences in manufacturing between MWT solar cells and conventional solar cells are the creation of through holes and the isolation and metallization wrap through from the front of the solar cell to the back of the solar cell. The manufacturing process for through holes has been developed and described during Phase I of this research program. The following chapter will focus on the isolation and metallization process.

2.2 Isolation

MWT solar cells require a more sophisticated approach to junction isolation than conventional H-bar solar cells. This is mainly due to the presence of a p-n junction at the walls of the through holes after diffusion. During Phase II of this program, we have evaluated three isolation concepts using either lasers to cut through the p-n junction on the back or using a chemical etch to remove the p-n junction on the entire back of the solar cell

2.2.1 Laser trench isolation

Laser trench isolation represents the most straightforward approach. The through holes can be isolated along with the wafer edges using an automated laser with a modified program. In this approach, we are isolating the n-type regions around the through holes from the p-type bulk by cutting a laser trench through the n+ region on the back between the aluminum back contact metal and the Ag front contact. The through hole edges will act like a regular cell edge. Figure 12 shows a representation of this approach.

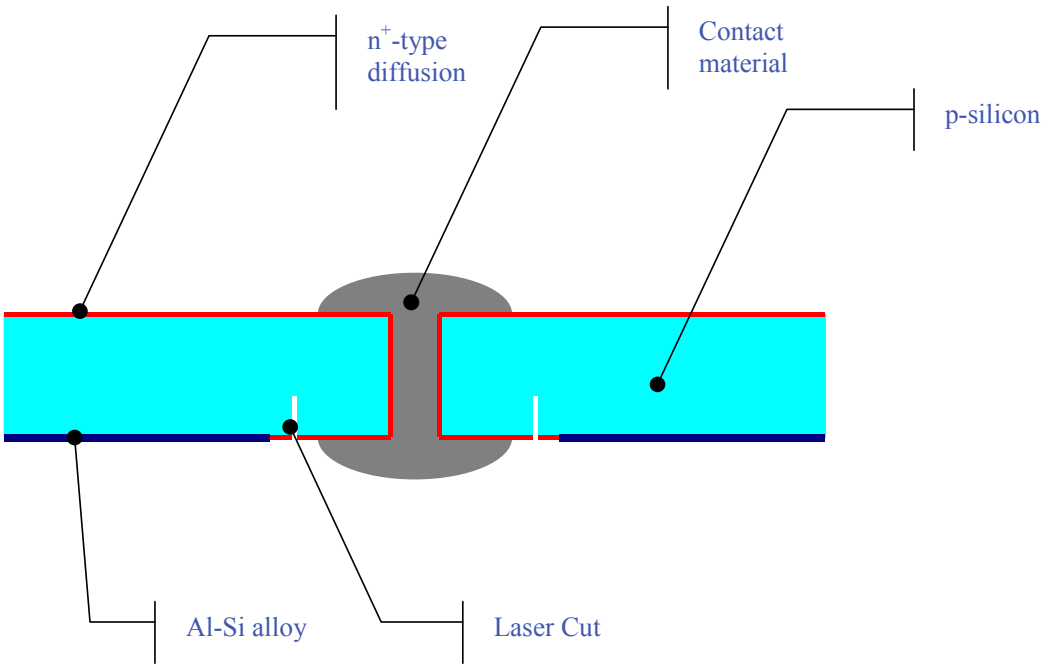

Figure 12 - Laser trench isolated MWT solar concept

This approach, while easily implemented, results in an alignment challenge. Tolerances required to ensure that the laser cut does not overlap with either the silver metal wrapped through from the front or the aluminum back contact metal have to be added to the dimension of the contact pads on the back. This creates a large area with no back contact where current has to travel laterally from the edge of the through hole to the edge of the aluminum back contact metallization. A reduction in fill factor can be the result.

2.2.2 Chemical isolation with epoxy filled though hole

A chemical backside isolation process that removes the p-n junction on the back of the wafer would isolate both the edge of the device and the through holes. This process removes not only the back junction but also the junction at the walls of the through holes creating a p-type area exposed to the wrap through metallization. To avoid shunting in this area, the front contact silver would be

printed only on the top of the wafer and the wrap through would be completed during the module manufacturing process using conductive adhesives in conjunction with the interconnect metal. Figure 13 shows a representation of the concept. This approach would result in a simplified solar cell process but the module assembly process would be more difficult and detract from the overall goal of a simplified and low cost module manufacturing process.

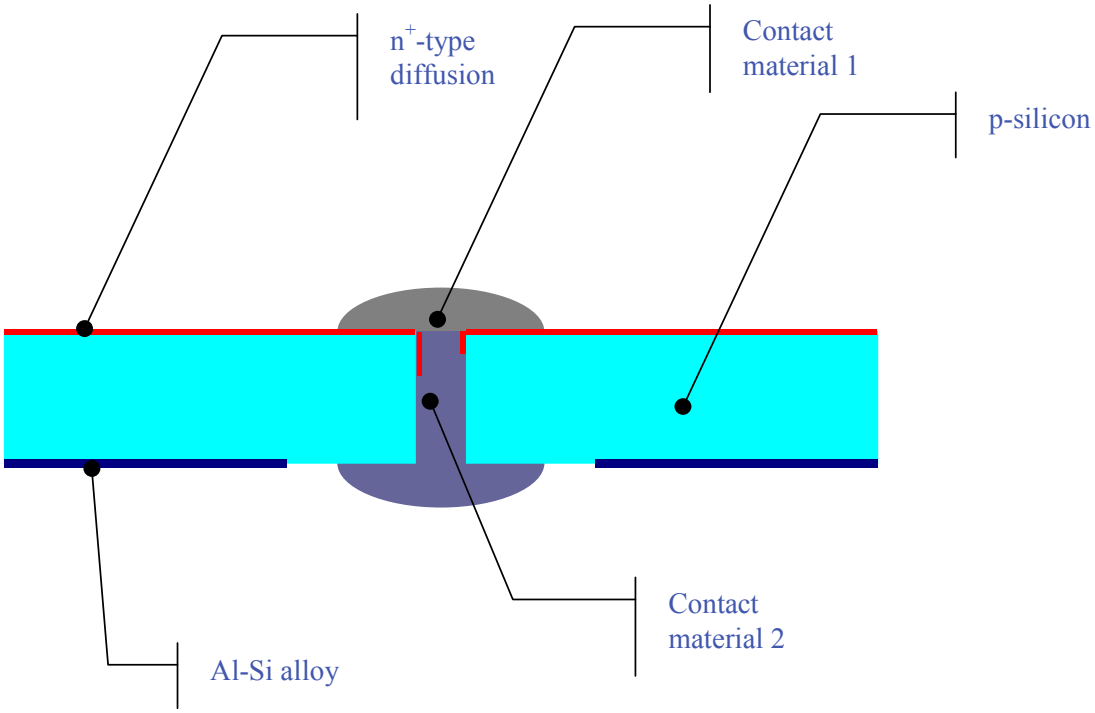

Figure 13 - Chemical back etch isolated MWT solar concept with two dissimilar contact materials

2.2.3 Chemical isolation with metal wrap through

This process would remove the back p-n junction as described in 2.2.2. However, in this case the silver metal would be wrapped through the hole despite the exposed base at the wall of the holes. The process relies on the poor contact screen printed silver will make with high resistive p-type silicon. Also the contact area is very small and leakage currents are relatively high in molded wafer solar cells due to the low lifetime of the material. Figure 14 shows a representation of the third approach. If shunting does not pose a significant problem this approach will result in both an easy solar cell manufacturing process and an easy module assembly process.

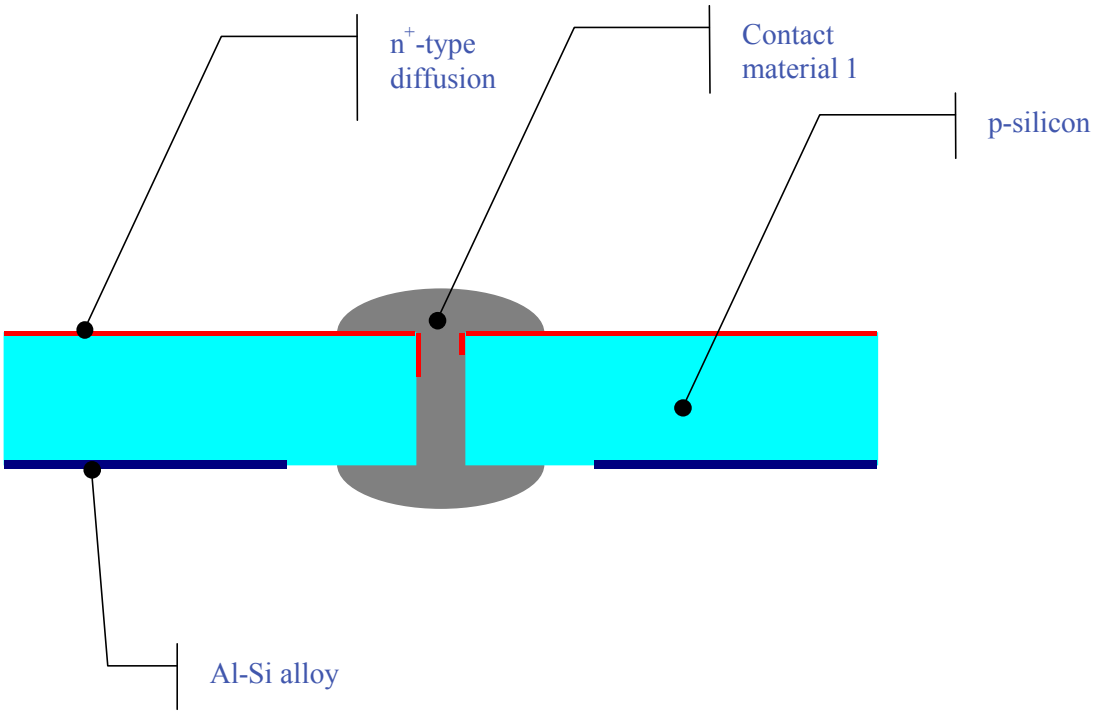

Figure 14 - Chemical back etch isolated MWT solar concept with single silver contact

To evaluate back etch isolation based approaches we installed and optimized an in-line back side etch prototype system from RENA. We used lock-in thermography to evaluate the effectiveness of the isolation process.

2.3 Metallization

We decided on a tapered bus-bar square sub-cell design for the front metallization. Modeling of resistive and shading losses resulted in an optimum of 16 through holes per 156 mm x 156 mm solar cell. The relatively low number of through holes is due to a combination of low short circuit current as well as limitations in screen-printing. While the model predicts lower losses with more than 16 though holes, the returns from increasing the number of through holes are increasingly diminished and very fine gridlines would be required to realize these gains. Figure 15 shows metallization related power loss as a function of number of though holes for our MWT solar cell design. Screens according to the design shown in Figure 16 were manufactured and tested.

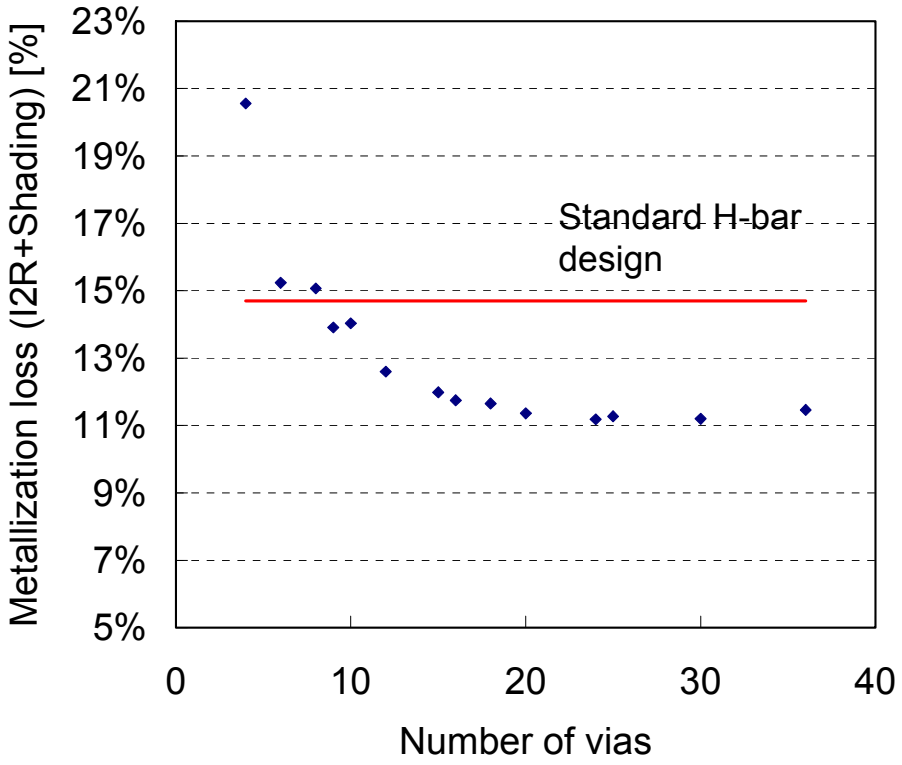

Figure 15 - Modeled loss for MWT solar cells

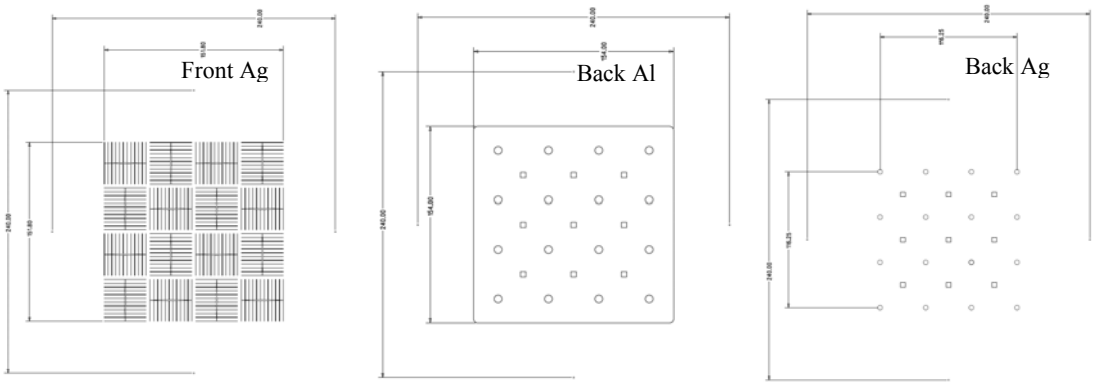

Figure 16 - MWT metallization design

2.4 Summary

In summary we modeled, optimized, and tested a MWT metallization design. We also evaluated three isolation concepts for through hole isolation.

3. Task 7 - Increased Solar Cell Efficiency and Yield - Advanced Cell Processing

3.1. Introduction

Molded wafer based solar cells have historically had low conversion efficiency. To improve the conversion efficiency both wafer quality and device quality need to be improved. Wafer quality was the focus of our effort during Phase I of this contract. In this task, efforts to improve the device quality are modification of emitter diffusion and silicon nitride deposition processes.

3.2 Diffusion Process

Changes to the emitter layer in silicon solar cells were investigated in an effort to improve the blue response of solar cells. The diffusion conditions used to create the n-type emitter layer were altered and the effect on the blue response determined. Three separate types of diffusion trials were conducted: 1) source limited diffusion trials, 2) diffusion temperature trials and 3) diffusion drive-in time trials. In all trial types, it was found that emitters having a sheet resistance less than 60 ohms/square gave an inferior blue response compared to more resistive emitters. Additionally, increasing the emitter sheet resistance beyond 80 ohms/square yielded no further improvements in blue response; the beneficial effects saturate beyond this resistance.

Texture etched multicrystalline solar cells were diffused using a range of process parameters, the device was then completed by depositing a Si_3N_4 antireflective coating and screen printing and firing metal contacts. Improvements in blue response were determined using internal quantum efficiency (IQE) measurements. The IQE is extracted from the reflectance and external quantum efficiency measurements. The blue response of the cells is determined from the IQE curves as depicted in Figure 16 below.

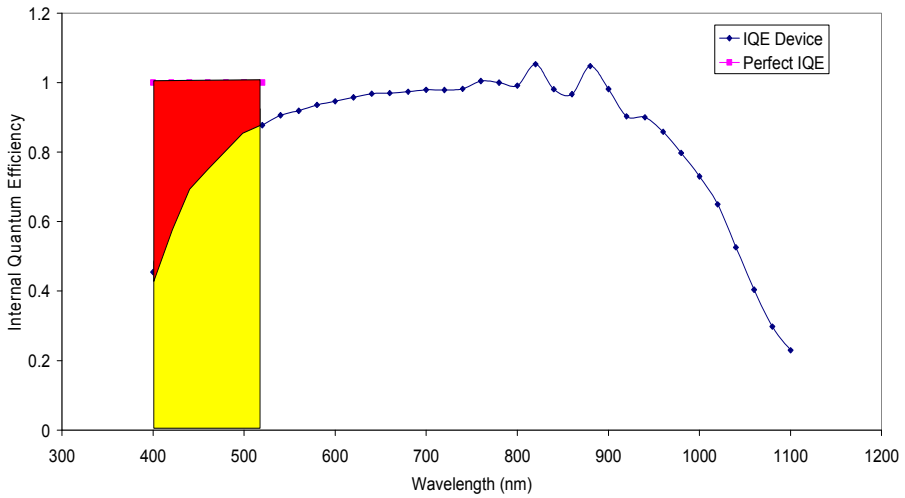

Figure 16 - Internal quantum efficiency curve for a solar cell

The fraction of the red rectangle obscured by the area under the IQE curve (shown in yellow) between 400 nm and 520 nm for the device is used as a measure of the blue response for a cell.

In Figure 16, the blue response is measured as the deviation from perfect IQE (i.e. IQE=1) between 400 nm and 520 nm. For illustration's sake, the area under the IQE curve in the blue response region is shaded in yellow. This yellow shaded region is partially obscuring the red rectangle behind it. This red rectangle represents the best possible blue response. The ratio of the area under the IQE curve of the device in question and an ideal device will give a number between 0 and 1 depending on the quality of the blue response. A value of 0 is translated as no blue response and 1 is an ideal blue response. This criteria was used to access the effectiveness of the various emitters created for this study.

3.2.1 Temperature Trials

In this section, the temperature used for the diffusion and drive in steps was varied, all other variables were kept constant. Table 3 gives the temperatures of these three trials along with the resulting emitter sheet resistance and cell blue response.

Trial	Temperature (°C)	Sheet Resistance ($\Omega/\square$)	Blue Response
A	High Temp	40	0.84
B	Medium Temp	60	0.904
C	Low Temp	75	0.963

Table 3 - Temperature Trial Conditions and Results

For Trials A, B, and C the $POCl_3$ flow rate was at a high level for the duration of the diffusion step. An additional drive-in diffusion followed termination of the active $POCl_3$ diffusion step. Note the increasing blue response with increasing emitter resistance in Table 3.

3.2.2 Source Limited Trials

In the source-limited trials, the flow rate of the n-type dopant source was varied while all other variables were held constant. There was no separate drive-in step used in these trials.

Table 4 gives the details of the source limited diffusion trials and the resulting blue response. All diffusions in this trial were carried out at a high temperature with no separate drive in step ($POCl_3$ flowing throughout diffusion). Figure 17 below shows the IQE curves for the source limited diffusion trials. There is a general trend of increased blue response with increasing emitter sheet resistance.

Trial	$POCl_3$ (sccm)	Sheet Resistance ($\Omega/\square$)	Blue Response
P	21x Low Flow	35	0.72
O	2.25x Low Flow	55	0.965
F	1.75x Low Flow	50	0.946
E	1.4x Low Flow	70	1
L	Low flow	105	1

Table 4 - Source Limited Trial Conditions and Results

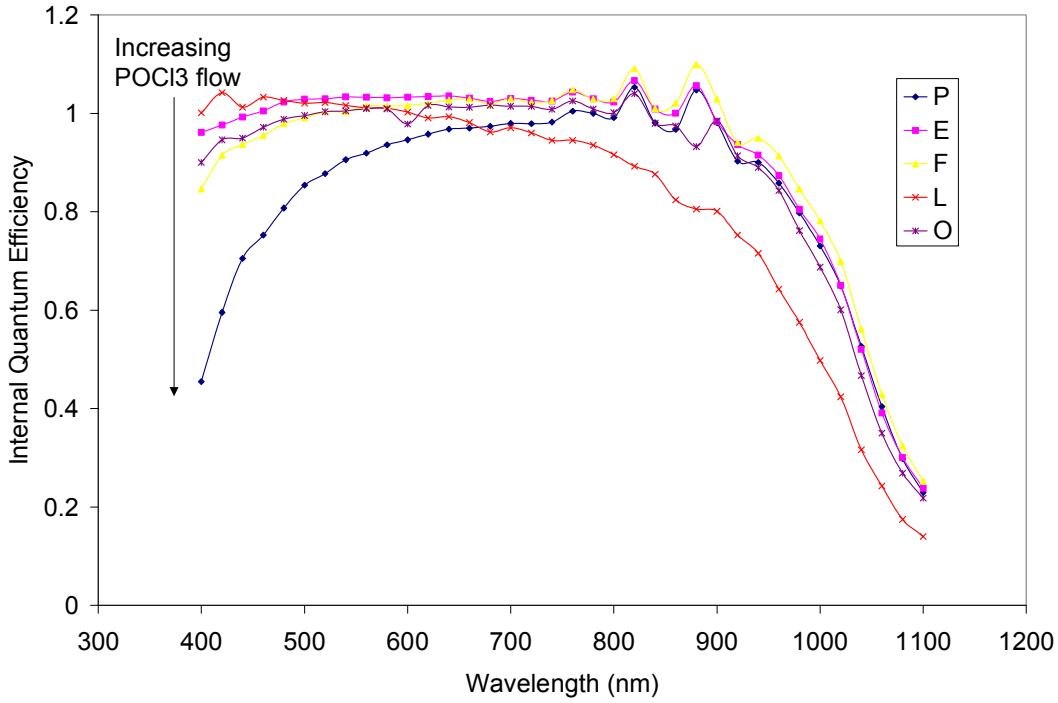

Figure 17 - IQE curves for the source limited diffusion trials

3.2.3 Drive-In Time Trials

In the final set of trials, the duration of the diffusion drive-in step was varied while all other diffusion variables were held constant. Table 5 below gives the details of the drive-in trials along with the resulting emitter sheet resistance and cell blue response. In the drive-in time trials, all diffusions were carried out at a high temperature with a high $POCl_3$ flow rate. Note the recurring theme of increasing blue response with increasing emitter sheet resistance/decreasing drive-in time. Figure 18 below shows the IQE curves measured for the cells in the drive-in time trial.

Trial	Drive-in Time	Sheet Resistance (Ω/□)	Blue Response
N	Long time	27.5	0.75
I	Medium time	42.5	0.81
G	Short time	50	0.86

Table 5 - Drive-In Trial Conditions and Results

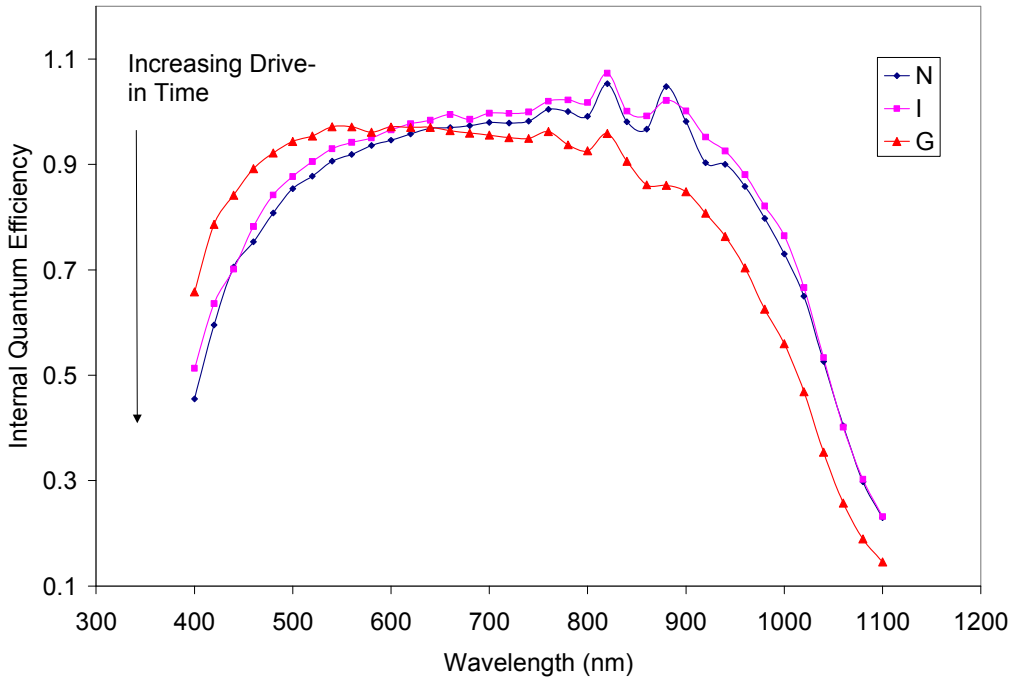

Figure 18 - IQE curves for the diffusion drive-in time trial

In Figure 18, the same general trend as the previous diffusion trials is seen. With decreasing drive-in time, an increasing sheet resistance of the emitter and a corresponding increase in the blue response of the resulting solar cells is present. However, this effect is less apparent in this trial since truly high emitter resistances were not achieved.
It is expected that the same trial conducted at lower temperatures would result in improved blue-responses.

3.2.4 Discussion

In an effort to bring the overall results of this emitter diffusion study into focus, the blue-response of each of the trials has been plotted as a function of emitter resistance in Figure 19. It is clear from this figure that all of the trials result in increasing blue-response with increasing emitter resistance. However, increasing the emitter sheet resistance to very high values is not without complications. As sheet resistance increases, the density of emitter gridlines must be increased to avoid series resistance losses in the resistive emitter. With increase gridline density, gridline width must be reduced to prevent excessive shading. Additionally, making a good ohmic contact becomes increasingly demanding as emitter resistance increases.

Because of the negative implications of increasing emitter sheet resistance discussed above, it is logical to choose the emitter that gives a good blue-response at the lowest possible sheet resistance. Examination of Figure 19

reveals that source limited diffusion trials were able to yield blue-responses better than 0.95 for sheet resistance as low as 55 ohms/sq.

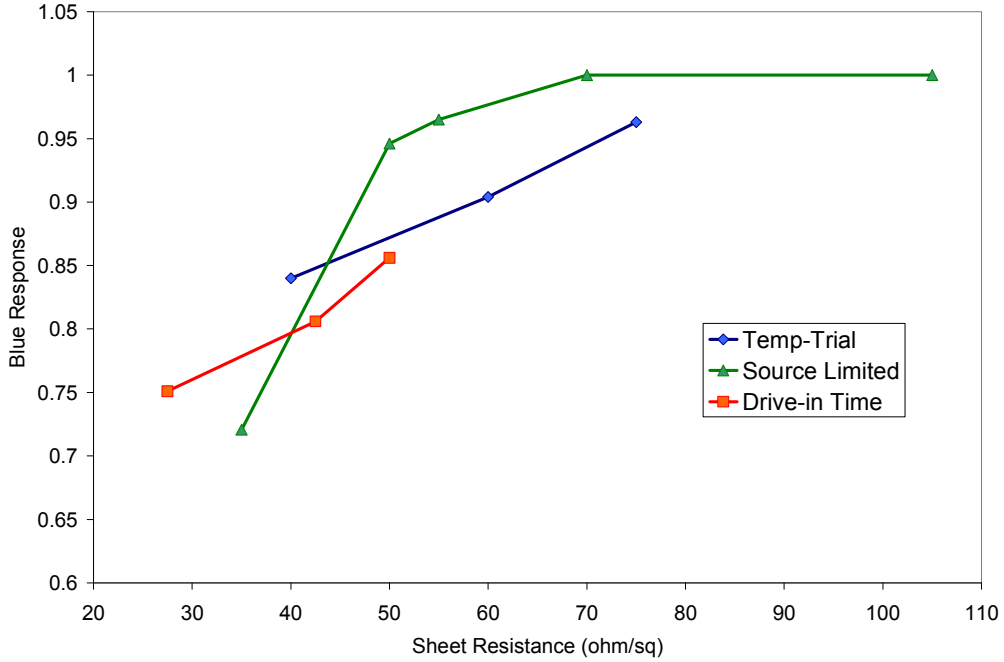

Figure 19 - Blue response as a function of emitter sheet resistance for the various diffusion trials

It is likely that the source limited diffusion trials have reduced phosphorus content at the surface (making surface passivation more effective) and also maintain a surface field that enhances carrier collection near the emitter surface. The other diffusion trials, which incorporate a separate drive-in step, require greater than 70 ohms/square emitters to achieve a blue-response comparable to the 55 ohm/square source limited diffusion emitter.

3.2.5 Conclusion

The emitter diffusion studies discussed herein highlight the strong dependence of solar cell blue response on emitter sheet resistance. It has been demonstrated that achieving an adequate blue response from cells with emitter sheet resistances below 55 ohm/square is not likely. Of the three diffusion trial attempted here (Diffusion temperature trial, diffusion drive-in time trial, and source limited diffusion), it was found that source limited diffusion profiles show the most promise for achieving solar cells with a good blue-response without raising the emitter sheet resistance to unpractical high values. It should be noted that enhancements of blue-response quickly saturate as emitter resistance surpasses 80 ohm/square (see Figure 19). Future studies will concentrate on source limited diffusion trials at approximately 60-70 ohm/square. It is likely an emitter screen redesign with a higher gridline density and a different emitter ink and firing profile will be required to achieve an optimal cell with this new emitter

diffusion profile. The 62-gridline emitter pattern used in this study showed increased series resistance losses with emitters greater than 60 ohm/square.

3.3 Silicon Nitride Antireflective Coating Optimization

Silicon Nitride optimization work was began during Phase II of this program but not completed due to the early termination of the contract. Nevertheless, silicon nitride optimization experiments were designed and partially carried out.. Specifically, potential performance enhancements using a graded silicon nitride layer were investigated.

3.3.1 Graded Silicon Nitride Layers

In this approach, silicon nitride will be produced in which the refractive index of the antireflection coating is graded from a high value at the silicon/SiN interface to a low value at the SiN/EVA or air interface. This is shown schematically in Figure 20 below.

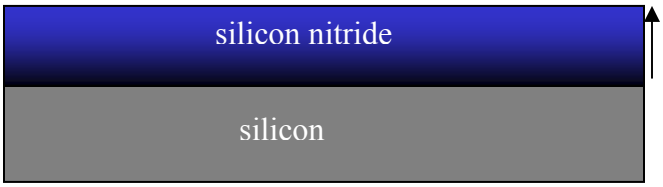

Figure 20 - SiN refractive index is decreasing in the direction of the arrow

The logic behind the graded approach is a reduction of the index mismatch at each interface light encounters as it crosses the EVA/SiN and SiN/Si interface. The refractive index of EVA (the plastic which encapsulates the solar cell) is approximately 1.47 while the index of silicon is 3.5 or greater depending upon wavelength being considered. Ideally, , the refractive index of the silicon nitride could be graded from 3.5 at the silicon surface, to 1.47 at the silicon nitride/EVA interface. Unfortunately, the range of refractive index achievable for SiN does not span this range. Values anywhere from 2.0 to 2.3 can be achieved in SiN. The expected performance benefit of this nitridation scheme, consider the following formula for normal reflectance at a single interface:

$$R = \left| \frac{n_2 - n_1}{n_2 + n_1} \right|^2 \qquad \text{(Eq. 1)}$$

For a two-interface system, such as that of a solar cell with an antireflection coating, the following formulation can be used to predict the fraction of light transmitted into the solar cell (interference effects not included here):

$$T = (1 - R_1)(1 - R_2) \qquad \text{(Eq. 2)}$$

Where:

T is the fraction of incident light transmitted into the solar cell
R_1 is the fraction of light reflected at the EVA/SiN interface
R_2 is the fraction of light reflected at the SiN/Silicon interface

In Figure 21 the transmittance of the EVA/SiN/Si optical system is given for all possible variations in refractive index of SiN between the Si and EVA interfaces according to Equation 2. The practically achievable transmittance range values are further limited by the deterioration of SiN's optical transparency for films having indices of refraction greater than 2.1. This usable region is the region contained within the black rectangular area of Figure 21.

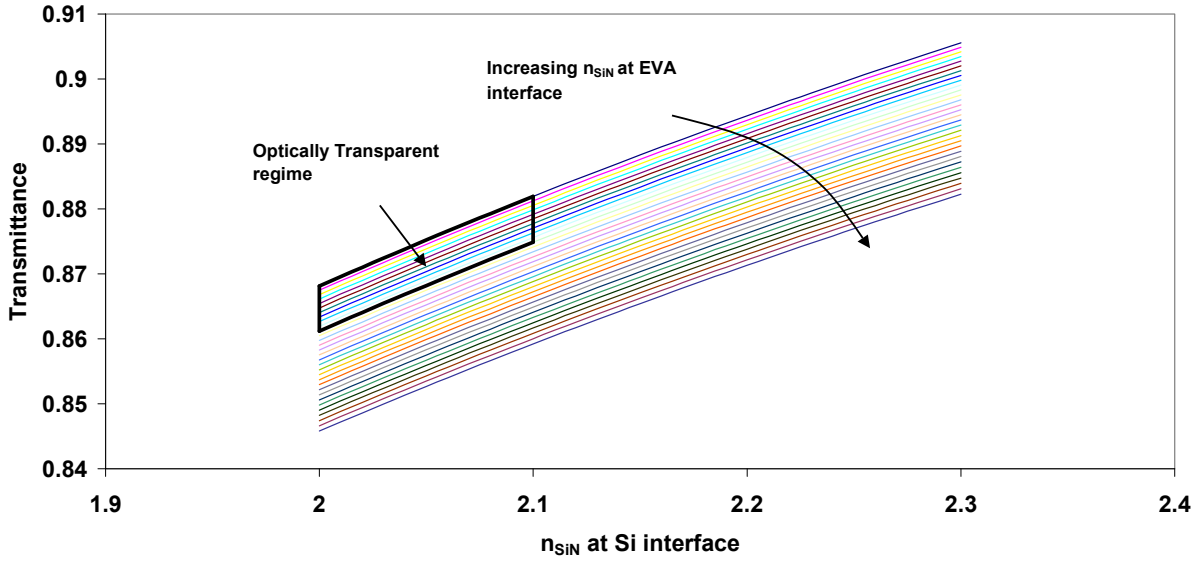

Figure 21 - Transmittance of the EVA/SiN/Si optical system for all possible combinations of SiN at the EVA and Si interfaces.

The best transmittance, ~88%, is achieved by varying n_{SiN} from 2.1 at the Si/SiN interface to 2.0 at the EVA/SiN interface.

4. Acknowledgements

This program is supported by the U.S. Department of Energy, National Renewable Energy Laboratory, PV Manufacturing R&D Project under Subcontract No. ZAX-5-33628-06.

REPORT DOCUMENTATION PAGE

Form Approved
OMB No. 0704-0188

PLEASE DO NOT RETURN YOUR FORM TO THE ABOVE ORGANIZATION.

1. REPORT DATE *(DD-MM-YYYY)*	2. REPORT TYPE	3. DATES COVERED *(From - To)*
June 2008	Subcontract Report	October 2005-September 2007

4. TITLE AND SUBTITLE
Solar Cell Design for Manufacturing; Final Report, October 2005 - September 2007

5a. CONTRACT NUMBER
DE-AC36-99-GO10337

5b. GRANT NUMBER

5c. PROGRAM ELEMENT NUMBER

6. AUTHOR(S)
J.A. Rand

5d. PROJECT NUMBER
NREL/SR-520-43228

5e. TASK NUMBER
PVB75301

5f. WORK UNIT NUMBER

7. PERFORMING ORGANIZATION NAME(S) AND ADDRESS(ES)
GE Energy, LLC
Newark, Delaware

8. PERFORMING ORGANIZATION REPORT NUMBER
ZAX-5-33628-06

9. SPONSORING/MONITORING AGENCY NAME(S) AND ADDRESS(ES)
National Renewable Energy Laboratory
1617 Cole Blvd.
Golden, CO 80401-3393

10. SPONSOR/MONITOR'S ACRONYM(S)
NREL

11. SPONSORING/MONITORING AGENCY REPORT NUMBER
NREL/SR-520-43228

12. DISTRIBUTION AVAILABILITY STATEMENT
National Technical Information Service
U.S. Department of Commerce
5285 Port Royal Road
Springfield, VA 22161

13. SUPPLEMENTARY NOTES
NREL Technical Monitor: Richard L. Mitchell

14. ABSTRACT *(Maximum 200 Words)*
Under this U.S. Department of Energy subcontract, GE Energy made significant progress in the following: (1) improving its solar cell process, (2) developing its metal wrap-through process, and (3) completing highly accelerated lifetime testing on elements of its roof-integrated module. In particular, GE improved its diffusion process, which resulted in near-ideal blue response at moderately low emitter sheet resistances of 50 to 60 ohms/sq. This result is important for GE's molded wafer development because of limited long-wavelength response.

15. SUBJECT TERMS
PV; manufacturer; silicon wafer; solar cells; module; back contact; metal wrap through; conversion efficiency

16. SECURITY CLASSIFICATION OF:			17. LIMITATION OF ABSTRACT	18. NUMBER OF PAGES	19a. NAME OF RESPONSIBLE PERSON
a. REPORT	b. ABSTRACT	c. THIS PAGE			
Unclassified	Unclassified	Unclassified	UL		19b. TELEPHONE NUMBER (*Include area code*)

Standard Form 298 (Rev. 8/98)
Prescribed by ANSI Std. Z39.18